Biochemical and Biophysical Research Communications 443 (2014) 749–755

Contents lists available at ScienceDirect

Biochemical and Biophysical Research Communications

journal homepage: www.elsevier.com/locate/ybbrc

Indatraline inhibits Rho- and calcium-mediated glioblastoma cell motility and angiogenesis

Jin-Chul Heo [a], Tae-Hoon Jung [a,b], Dae-Young Jung [a], Woo Kyu Park [a], Heeyeong Cho [a,*]

[a] Pharmacology Research Group, Drug Discovery Division, Korea Research Institute of Chemical Technology (KRICT), 141 Gajeong-ro, Yuseong, Daejeon 305-343, Republic of Korea
[b] Pharmacology Research Medicinal and Pharmaceutical Chemistry, University of Science and Technology (UST), 217 Gajeong-ro, Yuseong-gu, Daejeon 305-343, Republic of Korea

ARTICLE INFO

Article history:
Received 21 November 2013
Available online 12 December 2013

Keywords:
Indatraline
Glioblastoma multiforme
Proneural
Rho-GTP

ABSTRACT

Glioblastoma multiforme (GBM) is the most common and lethal primary brain tumor of the central nervous system (CNS). As an attempt to identify drugs for GBM therapeutics, phenotypic assays were used to screen 1000 chemicals from a clinical compound library. GBM subtypes exhibited different capabilities to induce angiogenesis when cultured on Matrigel; proneural cells migrated and formed a tube-like structure without endothelial cells. Among the compounds screened, indatraline, a nonselective monoamine transporter inhibitor, suppressed these morphological changes; it dose dependently inhibited cell spreading, migration, and *in vitro/in vivo* tube formation. In addition to intracellular calcium concentration, indatraline increased the level of Rho GTPase and its activity. Moreover, indatraline downregulated angiogenesis-related genes such as IGFBP2, PTN, VEGFA, PDGFRA, and VEGFR as well as nestin, a stem cell marker. These findings collectively suggest that the activation of Rho GTPase and the suppression of angiogenesis-related factors mediate the antiangiogenic activity of indatraline in proneural GBM culture.

1. Introduction

Glioblastoma multiforme (GBM) is the highest grade glioma variant and the most malignant and aggressive type of brain tumor [1]. In spite of intensive treatment including surgery, radiation, and chemotherapy, the mean life expectancy for patients with GBM is still <14 months [2]. Gliomas are classified into astrocytoma, oligodendroglioma, ependymoma, and mixed gliomas on the basis of the original cell types [3]. On the other hand, GBMs are classified into proneural, neural, classical, and mesenchymal subtypes according to gene expression profiles. Proneural cells showed a strong upregulation of the gene expression of platelet-derived growth factor (PDGF), PDGF receptor (PDGFR), and its downstream pathway [4]. The specific pathogenesis of proneural GBM has been intimately associated with PDGF signaling [5].

Recent studies have identified specific therapeutic targets for GBM treatment. Aspirin causes apoptosis via downregulation of IL-6-dependent STAT3 signaling in glioblastomas [6]. Harmine hydrochloride inhibits Akt phosphorylation in glioblastoma cells [7]. Histone deacetylase inhibitor and Wnt/β-catenin/Tcf signaling modulater inhibits the growth of glioblastoma cells [8,9].

To screen for antiangiogenic compounds, we evaluated the inhibitory activities of drug libraries against tube formation in three GBM subtypes. Among the noncytotoxic library compounds, indatraline showed the most potent antiangiogenic effect on proneural GBM. Until now, the pharmacological activities of indatraline on GBMs have not been documented precisely. Therefore, the present study aimed to investigate the antiangiogenic activities of indatraline in order to reveal its potential for GBM treatment.

2. Materials and methods

2.1. Materials

Indatraline [(1*R*,3*S*)-3-(3,4-dichlorophenyl)-*N*-methyl-2,3-dihydro-*1H*-inden-1-amine, chemical structure shown in Fig. 1B] and retinoic acid were obtained from Sigma Aldrich.

2.2. GBM tissue and primary cell culture

GBM patient samples were obtained from Samsung Medical Center (Seoul, Korea) after obtaining written informed consent from the patients in accordance with the appropriate Institutional

Abbreviations: GBM, glioblastoma multiforme; IGFBP2, insulin-like growth factor-binding protein 2; PDGFRA, platelet-derived growth factor receptor alpha; PTN, pleiotropin; VEGFA, vascular endothelial growth factor A; VEGFR, vascular endothelial growth factor receptor.

* Corresponding author. Fax: +82 42 861 4246.
E-mail address: hycho@krict.re.kr (H. Cho).

0006-291X/$ - see front matter © 2013 Elsevier Inc. All rights reserved.
http://dx.doi.org/10.1016/j.bbrc.2013.12.046

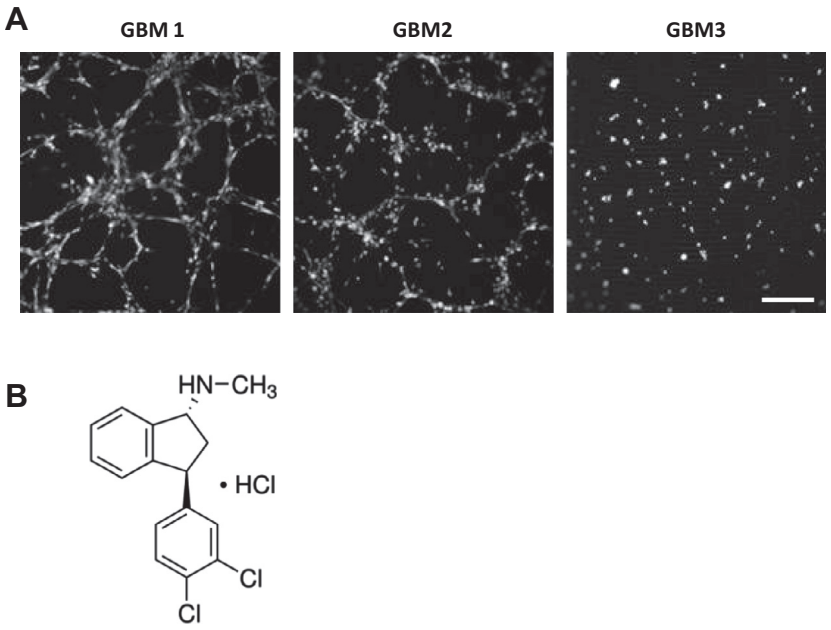

Fig. 1. Tube formation ability of three GBM subtypes and chemical structure of indatraline. (A) Capillary-like tube formation in three GBM subtypes (Scale bar = 200 μM). (B) Chemical structure of indatraline.

Review Boards. Tumors were classified by pathologists as GBM on the basis of WHO criteria [10].

Surgically isolated tumor tissues were mechanically dissected, followed by enzymatic dissociation and single cells purification, as reported previously [11]. Isolated cells were cultured under stem cell culture conditions in Neurobasal media with N2 and B27 supplements (Invitrogen) and human recombinant bFGF and EGF (R&D Systems). The cells were maintained in a ultra-low attachment flask (Corning) at 37 °C with 5% CO_2 and 95% air.

2.3. Oris cell migration assay

A migration assay was performed using the Oris Cell Migration Assay System (Platypus Technologies, USA) [12]. Stoppers were inserted into each well of a laminin/fibronectin-coated plate to prevent the attachment of the cells to the center of the well. The cells were seeded at 100 μL/well and incubated for 24 h to permit cell adhesion. After the cells had reached 90% confluence, the silicone stoppers were removed and indatraline (1–10 μM) was added to the cells. After 24 h, migration images were acquired using a microscope, and the migrated cells were quantified using Cellomics (Thermo) after Hoechst staining.

2.4. Tube formation assay

The 48-well plates were coated with 200 μL of growth factor-reduced BD Matrigel (10 μg/mL) and were polymerized by incubating at 37 °C for 2 h. Indatraline-treated cells (density, 5×10^4 cells/well) were suspended in Neurobasal-A medium present in the Matrigel-coated wells and incubated at 37 °C for 18 h. Antiangiogenic activity was calculated by measuring the angiogenic index using a Cellomics Array Scan [13].

2.5. Cell spreading assay

Cell adhesion was measured using an xCELLigence real-time cell analyzer (Roche) according to the manufacturer's protocol. Cell attachment and spreading was automatically analyzed by registering the electrical impedance of cell spreading on the laminin/fibronectin-coated plate [14].

2.6. Imaging of actin and vinculin

Cells were plated at a density of 2×10^4 cells/well on amine-coated 96-well plates (BD) and were incubated overnight. Indatraline was added, and the plates were incubated for 1 h. Immunofluorescence staining for F-actin assembly was performed with rhodamine-phalloidin (Invitrogen), and followed by fixing with 4% (w/v) paraformaldehyde in phosphate-buffered saline (PBS). The cells were washed three times for 5 min with 0.05% (v/v) Tween 20 in PBS and permeabilized for 5 min with 0.1% Triton X-100 (v/v) in PBS at room temperature. Subsequently, the cells were washed and blocked with 1% (w/v) bovine serum albumin (BSA). Vinculin labeling was achieved by incubating the cells for 1 h with 1:500 diluted anti-vinculin antibody (Abcam) in 5% (w/v) BSA and then the secondary antibody (KPL DyLight) in the dark. Fluorescence images were obtained using Cellomics [15].

2.7. Western blot analysis

Nestin expression was assessed using Western blot analysis. Cells were lysed and centrifuged at 16,000*g*. Then, the supernatant was resolved by 12% SDS–PAGE and transferred to nitrocellulose membranes. The membranes were blocked for 1 h with 5% skim milk in Tween (0.05%)/PBS, incubated with the primary antibody, and detected using HRP-conjugated antibody. The resultant immunoreactive bands were visualized using a West Femto Chemiluminescent substrate (Thermo) [16].

2.8. Calcium mobilization assay

The Fluo-4 NW Calcium Assay Kit (Invitrogen) was used according to the manufacturer's instructions [17]. In brief, 5×10^4 cells/well in 96-well amine-coated plates (BD) were washed two times with calcium-free Hanks balanced salt solution supplemented with 20 mM HEPES. A Fluo-4 NW dye mix solution (100 μL) was added to the culture plate, and the plate was incubated for 45 min at 37 °C. The plate signal was measured immediately after indatraline treatment with or without adenosine 5′-triphosphate (ATP, 1 μM). Values for fluorescence were recorded for 100 s in every 3 s at ex 485/em 525 nm using FlexStation II (Molecular Device).

2.9. Rho activity test

The GTP-bound form of Rho was monitored using a Rho-GTP Activation Kit (Pierce) [18]. In brief, cell lysates were centrifuged at 16,000*g*, and the supernatant was incubated for 1 h at 4 °C with GST-Rhotekin-RBD loaded on a SwellGel Immobilized Glutathione Disk. The glutathione disk-bound proteins were solubilized with 2 × SDS loading buffer [125 mM Tris–HCl (pH 6.8), 2% glycerol, 4% SDS (w/v), 0.05% mercaptoethanol, and 0.05% bromophenol blue]. Isolated Rho-GTP protein from the disk was separated on 12% SDS–PAGE and analyzed by Western blot.

2.10. RNA extraction and qPCR

Trizol™ (Invitrogen) was used to extract RNA. Following reverse transcription, real-time PCR was performed using a QuantiTect SYBR Green PCR Kit (Qiagen) [19]. Template cDNA was mixed with SYBR Green master mix containing Taq and dNTPs (Qiagen), and each of forward and reverse primers. The primers used for PCR were 18S rRNA forward: 5′-CCT TGG ATG TGG TAG CCG TTT-3′, reverse: 5′-AAC TTT CGA TGG TAG TCG CCG-3′, vascular endothelial growth factor receptor-1 (VEGFR-1) forward: 5′-ACA ATC AGA GGT GAG CAC TGC AA-3′, reverse: 5′-TCC GAG CCT GAA AGT TAG CAA-3′, VEGF A (VEGFA) forward: 5′-GTG TGC GCA GAC AGT GCT CCA-3′, reverse: 5′-ACA GCA GAA AGT TCA TGG TTT CG-3′, PDGFR alpha (PDGFRA) forward: 5′-CTT CTC ACA GGG CTG AGC CTA-3′, reverse: 5′-TCC ACA TCG GAG CTC TCT TCT TC-3′, insulin-like growth factor-binding protein 2 (IGFBP2) forward: 5′-ATG ACC ACT CAG AAG GAG GCC-3′, reverse: 5′-CCA AGG TGA TGC TTG CCA CCC TT-3′ and pleiotropin (PTN) forward: 5′-ACC ATG AAG CAG AGA TGT AAG-3′, reverse: 5′-CTT GGA GAT GGT GAC AGT CTT CT-3′. qPCR was performed using a CFX96 Touch™ Real-Time PCR Detection System (Bio-Rad). All experiments were repeated three times. The related gene expression levels were analyzed after normalization to 18S mRNA.

2.11. Chick chorioallantoic membrane (CAM) assay

Fertilized chicken eggs were incubated at 37 °C in 80% humidified incubator. On the third day, 2 mL of albumin was aspirated from the eggs using a 22-gauge hypodermic needle to detach the developing CAM from the shell. On the fourth day, the shell was punched out to make windows, and a thermanox coverslip (Nunc) coated with 10 μL indatraline (10 μM) or with vehicle was applied to the CAM surface and sealed using a cellophane tape. Blood vessels were observed under the microscope after injection of Intralipid 10% in 2 days. Photographs were taken and the total length of the vessels was quantified using Cellomics (Thermo) [20].

2.12. Data analysis

Data were expressed as mean ± standard deviation (S.D.), and the differences between two groups were compared using paired Student's *t*-test. All experiments were performed and replicated in triplicates. *p* Values of $<0.01^{*}$ and $<0.001^{**}$ were considered significant.

3. Results

3.1. Indatraline inhibited the spreading and migration of GBM

The tube forming ability of GBM1–3 was compared on Matrigel. Among them, GBM1 (proneural subtype) showed stronger angiogenic activity than GBM2 (mesenchymal) and GBM3 (classical) (Fig. 1A).

A series of angiogenesis assays with indatraline manifested its antiangiogenic activities. Indatraline suppressed the spreading, migration, and tube formation of cultured GBM without cytotoxicity (Fig. 2D).

In spreading assays, indatraline 1, 3, and 10 μM inhibited the attachment and spreading ability of GBM1 in a dose- and time-dependent manner (Fig. 2A and C). Cell migration analysis also showed dose-dependent inhibition by indatraline (Fig. 2B and D).

3.2. Indatraline induced cytoskeletal collapse and inhibited the expression of proangiogenic factors

Cellular morphology is largely determined by events of actin filaments and microtubules. These cytoskeletal elements influence cell adhesion formation and morphology. To further characterize the effects of indatraline on cell shape, focal adhesion and cytoskeleton were examined using a fluorescence microscope. Indatraline caused a significant assembly of F-actin-containing stress fibers. Many cells displayed an aggregated and collapsed actin filament, which finally became rounded. Indatraline 5 and 10 μM also detached the focal adhesion molecule vinculin (Fig. 2E). Immunoblotting data revealed the inhibition of nestin expression in GBM1. Indatraline 5 μM treatment for 48 h decreased nestin expression by 60% (Fig. 2F and G). Reduced expression of nestin, a neural stem cell marker, indicates loss of stemness, which can correlate with neuronal or endothelial differentiation. According to the fact that indatraline can modify cell migration in proneural GBM, we hypothesized that indatraline might influence the expression of genes associated with cell migration. Real-time quantitative RT-PCR revealed the decreased transcript levels of IGFBP2, PTN, VEGFA, PDGFRA, and VEGFR, related angiogenesis and motility factor, in indatraline-treated GBM1 (Fig. 2H). These results indicate that indatraline inhibits cell migration and spreading through F-actin collapse and the expression of the glioblastoma progression marker, nestin. Moreover, indatraline suppressed the expression of proangiogenic factors in proneural GBM.

3.3. Indatraline induces calcium mobilization

Indatraline dose dependently induced an intracellular calcium flux in GBM1. Indatraline induced 12% and 29% increases in calcium at 10 and 30 μM, respectively (Fig. 3A). Moreover, indatraline and ATP combination treatment induced an additional increase in calcium concentrations compared with ATP alone treatment. Indatraline and ATP combination treatment induced 6%, 12%, and 20% increases in calcium concentrations at 1, 3, and 10 μM, respectively, compared with ATP alone treatment (Fig. 3B). These data indicate that the indatraline-induced increase in calcium concentrations may be produced by an ATP-independent mechanism.

3.4. Activation of the Rho pathway by indatraline

To gain insight into the mechanism of action of indatraline, we measured the amount of Rho-GTP in GBM1 in the presence of indatraline. Rho activity increased by 2.9- (1 μM), 3.7- (3 μM), and 4.0-fold (10 μM) after 15 min of indatraline treatment (Fig. 3C and E). However, the enhancement was transient and Rho activity was diminished to the basal level within 1 h (Fig. 3D and F).

3.5. Indatraline inhibited tube formation by proneural GBMs and angiogenesis in the CAM assay

Tube formation by proneural GBM cells was dose dependently suppressed with 1, 3, and 10 μM indatraline (Fig. 4A and C). The angiogenic index, which comprises tube length and node number,

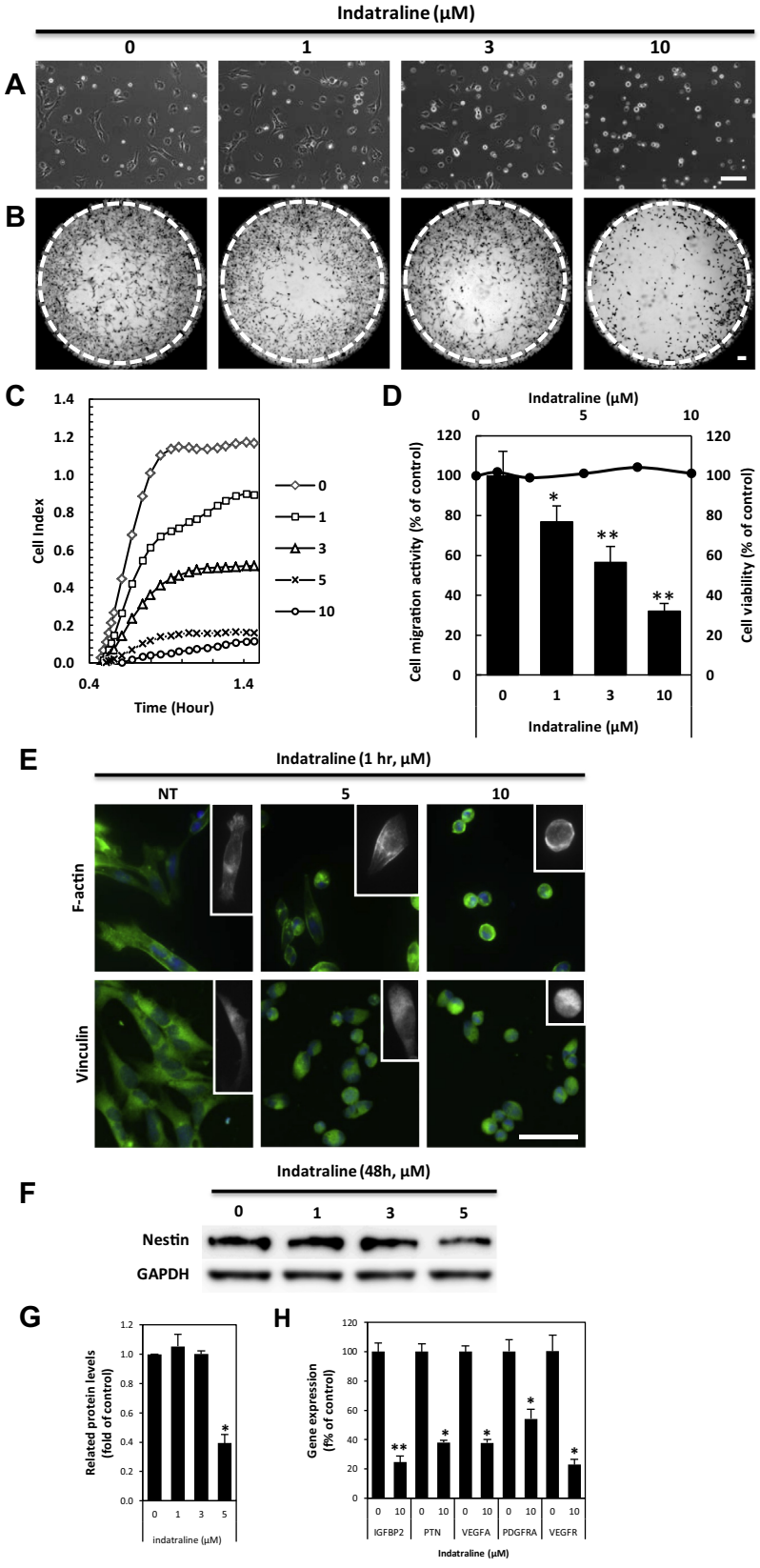

Fig. 2. Indatraline inhibited cell motility and related gene expression in proneural GBM. (A) Spreading was measured in GBM exposed to various concentration of indatraline for 1 h. (B) To determine migration activity in the Oris cell migration assay. (C) Time-dependent quantitative evaluation of GBM adhesion in response to indatraline using the xCELLigence system. (D) Quantitative measurement of cell migration activity and cell viability by indatraline. (E) Indatraline induced actin and adhesion complex detachment in GBM. Cells were fixed and stained for F-actin and the focal adhesion protein vinculin. (F) Western blot analysis of nestin expression using GBM cells treated with indatraline for 48 h. (G) Quantification of nestin expression by indatraline. (H) Relative expression level of IGFBP2, PTN, VEGFA, PDGFRA, and VEGFR mRNA measured by RT-qPCR in GBM cells treated with indatraline (10 μM). All experiments were performed in triplicates. Scale bar represent 100 μM. Data represent mean ± S.D. compared with the data for the DMSO control cells. Significant difference from the control, $^{*}p < 0.01$ and $^{**}p < 0.001$.

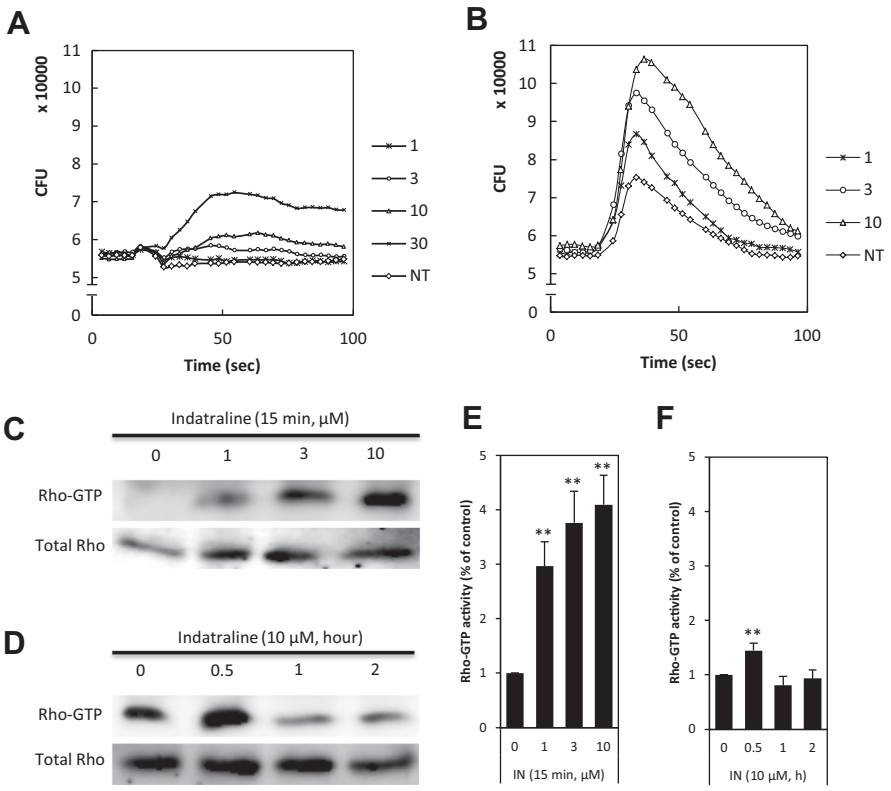

Fig. 3. Indatraline increased intracellular calcium concentrations and Rho activity in proneural GBM. (A) Intracellular calcium mobilization was increased in a dose-dependent manner when GBM were treated with titrated concentrations of indatraline. (B) Indatraline and ATP combination treatment increased intracellular calcium concentrations in a dose-dependent manner in GBM (NT, no treatment and DMSO control). (C) Rho was activated by indatraline in a dose-dependent manner. (D) Rho activation was depending on the time. (E) Quantification of Rho-GTP expression against concentration of indatraline. (F) Quantification of Rho activation by treatment interval of indatraline (IN). Data represent mean ± S.D. compared with the data for the DMSO control cells. Significant difference from the control, $^{**}p < 0.001$.

decreased by 23% (1 μM), 56% (3 μM), and 98% (10 μM) with indatraline.

Furthermore, we found that indatraline strongly inhibited the formation of new vessels on CAM as observed in the inhibitory control group treated with retinoic acid. After 2 days of treatment, retinoic acid at 1 μg/egg showed approximately 40% inhibition in the branching numbers of blood vessels. When indatraline was applied at 10 μg/egg on CAM, angiogenesis inhibition was estimated to be 48% (Fig. 4B and D), which clearly indicates that indatraline has potent antiangiogenic activity.

4. Discussion

Sprouting new blood vessels from an existing vascular structure is a complex and essential procedure for the survival of tumors. In this study, we found a potent inhibitor of cell motility and angiogenesis. Indatraline is a nonselective monoamine transporter agent [21]. Until now, the pharmacological activities of indatraline on proneural GBM have not been documented precisely. We here clarified the antiangiogenic activities of indatraline using both *in vitro* and *in vivo* models.

Many researchers have reported drugs that reduce angiogenesis in brain tumors. Atorvastatin reduced the protumorigenic effects of microglia on glioma migration and invasion by reducing the microglial expression of membrane type 1 metalloproteinase [22]. The antitumor activity of a small molecule polypeptide chemokine PK2 antagonist, PKRA7, in the context of glioblastoma [23] and Geldanamycins (inhibitors of HSP90) blocked glioblastoma growth [24]. In search of antiangiogenic compounds, we used spreading, migration, and tube formation assays, which are important phenotypic tools for monitoring cell motility particularly in cancer research. This study showed that indatraline inhibited cell motility in a dose-dependent manner (Figs. 2 and 4). Indatraline also inhibited tube formation in human glioblastoma U18MG cells and human umbilical vein endothelial cells (data not shown).

Several novel therapeutic targets are involved in the invasion and motility of GBM. Epidermal growth factor receptor pathway substrate 8 (Eps8) is a crucial regulator of the actin cytoskeleton dynamics accompanying cell motility and invasion in GBM [25]. Narciclasine, a plant growth modulator, showed activities related to cell proliferation, morphology, and actin cytoskeleton organization through the modulation of the Rho pathway in human GBM [26]. We measured adhesion signaling molecules and actin cytoskeleton rearrangement in proneural GBM. The effect of indatraline on F-actin organization was detectable under a microscope after F-actin and vinculin staining; collapse of stress fibers and detachment was observed (Fig. 2E).

Nestin, a class VI intermediate filament protein, was originally described as a neuronal stem cell marker during central nervous system development. Nestin expression was significantly higher in high-grade tumors from patient biopsies than in low-grade tumors [27]. Moreover, nestin plays important roles in cell growth, migration, invasion, and adhesion to extracellular matrices in glioma cells [28]. In the present study, indatraline (5 μM for up to 48 h) decreased nestin expression in proneural GBM (Fig. 2F and G).

Next, we examined the effects of indatraline on angiogenesis on the basis of the expression level of the angiogenesis-related genes IGFBP2, PTN, VEGFA, PDGFRA, and VEGFR. IGFBP2 is involved in GBM invasiveness and angiogenesis [29–31]. Our result explains

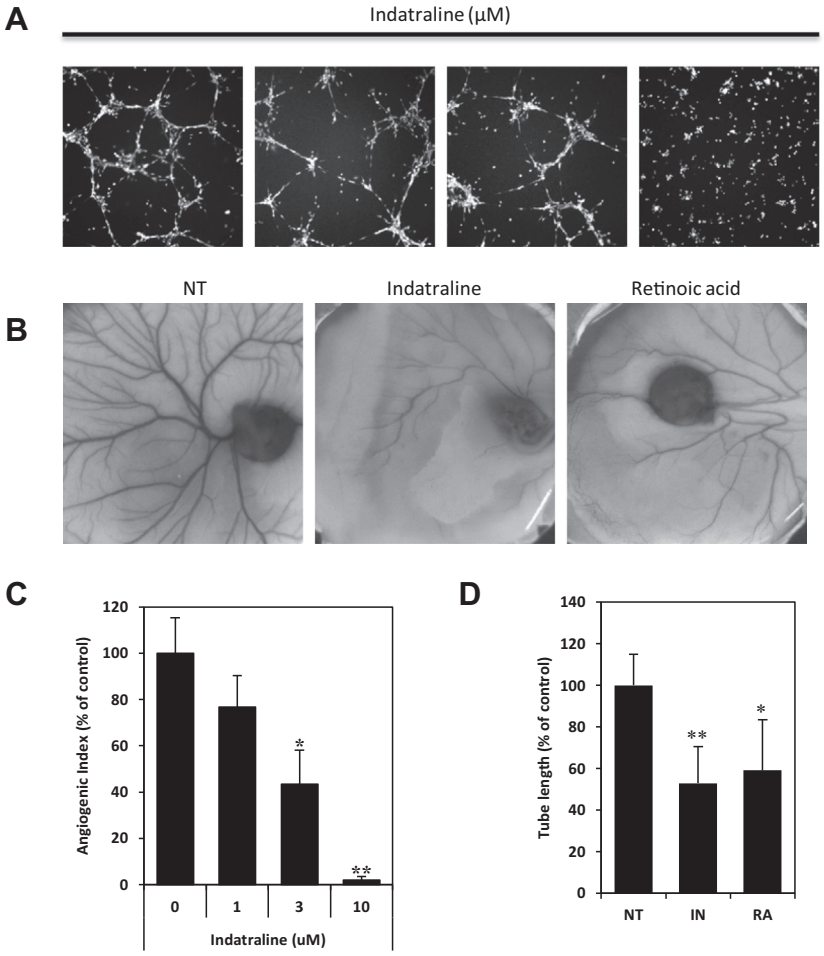

Fig. 4. The inhibitory effect of indatraline on angiogenesis-related genes and angiogenesis in proneural GBM. (A) Indatraline dose dependently inhibited capillary-like tube formation in GBM (Scale bar = 200 μM). (B) Inhibitory effects of indatraline on chick embryo chorioallantoic membrane (CAM) angiogenesis. Retinoic acid was used as a positive control. (C) Quantification of tube formation activity. (D) Quantification of angiogeneic activity in the CAM assay (NT, no treatment; IN, indatraline; RA, retinoic acid). Each column represents mean ± S.D. Significant difference from the control, $^{*}p < 0.01$ and $^{**}p < 0.001$.

that indatraline inhibited angiogenesis through the suppressed expression of IGFBP2, PTN, VEGFA, PDGFRA, and VEGFR in proneural GBM (Fig. 2H).

Cytoskeletal rearrangements including focal adhesion turnover induce changes in morphology during migration. Actin polymerization occurs within a dense meshwork of actin filaments that is important for cell motility. Calcium channels represent a specific channel family overexpressed in different types of tumors, and this signaling is important in many signaling processes involved in the proliferation and motility of cancer cells, including those of glioblastomas of the brain. They are involved in controlling the proliferation, angiogenesis, and invasion of tumor cells [32]. Calcium-activated protease calpain 2 regulates glioblastoma cell invasion by mediating adhesion and cytoskeletal plasticity [33]. Numerous studies showed that the increase in intracellular calcium concentrations was synchronized with the induced cell motility. However, the indatraline-induced increase in intracellular calcium concentrations (Fig. 3A and B) resulted in decreased motility.

The increase in calcium concentrations and Rho activity are very closely related. Actin remodeling at dendritic spines is dependent on the calcium and Rho GTPase signaling activity [34]. Rho activation is classically associated with the formation of actin stress fibers and is related to tumor cell motility and tumor progression. The GTPase signaling pathway presents innovative drug targets for glioma therapy [35]. Inhibition of glioma cell migration by sphingosine 1-phosphate is associated with RhoA activation and Rac1 suppression in glioblastoma cells [36]. Farnesyl thiosalicylic acid can avert the transformation of human GBM cells by inhibiting both their migration through decreased Rac-1 activity and RhoA activation [37]. Therefore, we examined the effect of indatraline on Rho-GTP levels in GBM. Indatraline increased Rho-GTPase activity in a dose-dependent manner, suggesting that indatraline has the potential to increase the Rho activity level (Fig. 3).

Angiogenesis is important in the development and progression of various pathological conditions including tumor growth and metastasis in GBM [38]. Downregulation of angiogenesis has been considered advantageous for the prevention of neoplastic growth and inflammation. The CAM assay was used for examining the inhibitory activity of indatraline, and retinoic acid was used as a positive control for the assay (Fig. 4B).

In conclusion, indatraline inhibited spreading, migration, and tube formation, suggesting both antimetastatic and antiangiogenic activities in GBM cells. In addition, signal transduction related to calcium and Rho signaling appeared to be the mechanism underlying the inhibitory activity of indatraline against GBM cell motility. These results also indicate that indatraline might have a therapeutic potential for GBM treatment.

Acknowledgments

This work was supported by a Grant from Korea Research council for Industrial science and Technology (KK-1303-D0) and the

Global Frontier Project Grant (NRF-MIAXA002-2010-0029776) of National Research Foundation funded by the Ministry of Education, Science and Technology of Korea. GBM patient samples used in this study were obtained from Dr. Do-Hyun Nam, Samsung Medical Center (Seoul, Korea).

References

[1] L.M. DeAngelis, Brain tumors, N. Engl. J. Med. 344 (2001) 114–123.
[2] R.V. Patwardhan, C. Shorter, B.K. Willis, et al., Survival trends in elderly patients with glioblastoma multiforme: resective surgery, radiation, and chemotherapy, Surg. Neurol. 62 (2004) 207–213.
[3] J.D. van der Meulen, H.J. Houthoff, E.J. Ebels, Glial fibrillary acidic protein in human gliomas, Neuropathol. Appl. Neurobiol. 4 (1978) 177–190.
[4] R.G. Verhaak, K.A. Hoadley, E. Purdom, et al., Integrated genomic analysis identifies clinically relevant subtypes of glioblastoma characterized by abnormalities in PDGFRA, IDH1, EGFR, and NF1, Cancer Cell 17 (2010) 98–110.
[5] J. Silber, A. Jacobsen, T. Ozawa, et al., MiR-34a repression in proneural malignant gliomas upregulates expression of its target PDGFRA and promotes tumorigenesis, PLoS One 7 (2012) e33844.
[6] S.R. Kim, M.K. Bae, J.Y. Kim, et al., Aspirin induces apoptosis through the blockade of IL-6-STAT3 signaling pathway in human glioblastoma A172 cells, Biochem. Biophys. Res. Commun. 387 (2009) 342–347.
[7] H. Liu, D. Han, Y. Liu, et al., Harmine hydrochloride inhibits Akt phosphorylation and depletes the pool of cancer stem-like cells of glioblastoma, J. Neurooncol. 112 (2013) 39–48.
[8] H. Jin, L. Liang, L. Liu, et al., HDAC inhibitor DWP0016 activates p53 transcription and acetylation to inhibit cell growth in U251 glioblastoma cells, J. Cell. Biochem. 114 (2013) 1498–1509.
[9] G.R. Sareddy, D. Kesanakurti, P.B. Kirti, et al., Nonsteroidal anti-inflammatory drugs diclofenac and celecoxib attenuates Wnt/Beta-catenin/Tcf signaling pathway in human glioblastoma cells, Neurochem. Res. 38 (2013) 2313–2322.
[10] D.N. Louis, H. Ohgaki, O.D. Wiestler, The 2007 WHO classification of tumours of the central nervous system, Acta Neuropathol. 114 (2007) 97–109.
[11] K.M. Joo, S.Y. Kim, X. Jin, et al., Clinical and biological implications of CD133-positive and CD133-negative cells in glioblastomas, Lab. Invest. 88 (2008) 808–815.
[12] W. Gough, K.I. Hulkower, R. Lynch, et al., A quantitative, facile, and high-throughput image-based cell migration method is a robust alternative to the scratch assay, J. Biomol. Screen. 16 (2011) 155–163.
[13] J.C. Heo, J.Y. Park, S.U. Woo, et al., Dykellic acid inhibits cell migration and tube formation by RhoA-GTP expression, Biol. Pharm. Bull. 29 (2006) 2256–2259.
[14] P.T. Witkowski, L. Schuenadel, J. Wiethaus, et al., Cellular impedance measurement as a new tool for poxvirus titration, antibody neutralization testing and evaluation of antiviral substances, Biochem. Biophys. Res. Commun. 401 (2010) 37–41.
[15] R. Maddala, V.N. Reddy, D.L. Epstein, et al., Growth factor induced activation of Rho and Rac GTPases and actin cytoskeletal reorganization in human lens epithelial cells, Mol. Vis. 9 (2003) 329–336.
[16] J.C. Heo, S.H. Lee, Alleviation of asthma-related symptoms by a derivative of L-allo threonine, Int. J. Mol. Med. 31 (2013) 881–887.
[17] R.A. Vongsa, N.P. Zimmerman, M.B. Dwinell, CCR6 regulation of the actin cytoskeleton orchestrates human beta defensin-2- and CCL20-mediated restitution of colonic epithelial cells, J. Biol. Chem. 284 (2009) 10034–10045.
[18] E.E. Govek, S.E. Newey, L. Van Aelst, The role of the Rho GTPases in neuronal development, Genes Dev. 19 (2005) 1–49.
[19] P.A. Geomela, C.K. Kontos, I. Yiotakis, et al., Quantitative expression analysis of the apoptosis-related gene, BCL2L12, in head and neck squamous cell carcinoma, J. Oral Pathol. Med. 42 (2013) 154–161.
[20] M.R. Youn, M.H. Park, C.K. Choi, et al., Direct binding of recombinant plasminogen kringle 1–3 to angiogenin inhibits angiogenin-induced angiogenesis in the chick embryo CAM, Biochem. Biophys. Res. Commun. 343 (2006) 917–923.
[21] M.S. Kleven, J.M. Kamenka, J. Vignon, et al., Pharmacological characterization of the discriminative stimulus properties of the phencyclidine analog, *N*-[1-(2-benzo(b)thiophenyl)-cyclohexyl]piperidine, Psychopharmacology (Berl) 145 (1999) 370–377.
[22] Y. Yongjun, H. Shuyun, C. Lei, et al., Atorvastatin suppresses glioma invasion and migration by reducing microglial MT1-MMP expression, J. Neuroimmunol. 260 (2013) 1–8.
[23] V.F. Curtis, H. Wang, P. Yang, et al., A PK2/Bv8/PROK2 antagonist suppresses tumorigenic processes by inhibiting angiogenesis in glioma and blocking myeloid cell infiltration in pancreatic cancer, PLoS One 8 (2013) e54916.
[24] K. Miekus, J. Kijowski, M. Sekula, et al., 17AEP-GA, an HSP90 antagonist, is a potent inhibitor of glioblastoma cell proliferation, survival, migration and invasion, Oncol. Rep. 28 (2012) 1903–1909.
[25] M.G. Cattaneo, E. Cappellini, L.M. Vicentini, Silencing of Eps8 blocks migration and invasion in human glioblastoma cell lines, Exp. Cell Res. 318 (2012) 1901–1912.
[26] F. Lefranc, S. Sauvage, G. Van Goietsenoven, et al., Narciclasine, a plant growth modulator, activates Rho and stress fibers in glioblastoma cells, Mol. Cancer Ther. 8 (2009) 1739–1750.
[27] T. Strojnik, G.V. Rosland, P.O. Sakariassen, et al., Neural stem cell markers, nestin and musashi proteins, in the progression of human glioma: correlation of nestin with prognosis of patient survival, Surg. Neurol. 68 (2007) 133–143. discussion 143-134.
[28] T. Ishiwata, K. Teduka, T. Yamamoto, et al., Neuroepithelial stem cell marker nestin regulates the migration, invasion and growth of human gliomas, Oncol. Rep. 26 (2011) 91–99.
[29] T. Fukushima, H. Kataoka, Roles of insulin-like growth factor binding protein-2 (IGFBP-2) in glioblastoma, Anticancer Res. 27 (2007) 3685–3692.
[30] U. Ulbricht, M.A. Brockmann, A. Aigner, et al., Expression and function of the receptor protein tyrosine phosphatase zeta and its ligand pleiotrophin in human astrocytomas, J. Neuropathol. Exp. Neurol. 62 (2003) 1265–1275.
[31] Y.H. Zhou, Y. Hu, D. Mayes, et al., PAX6 suppression of glioma angiogenesis and the expression of vascular endothelial growth factor A, J. Neurooncol. 96 (2010) 191–200.
[32] G. Santoni, M. Santoni, M. Nabissi, Functional role of T-type calcium channels in tumour growth and progression: prospective in cancer therapy, Br. J. Pharmacol. 166 (2012) 1244–1246.
[33] H.S. Jang, S. Lal, J.A. Greenwood, Calpain 2 is required for glioblastoma cell invasion: regulation of matrix metalloproteinase 2, Neurochem. Res. 35 (2010) 1796–1804.
[34] T. Saneyoshi, Y. Hayashi, The Ca^{2+} and Rho GTPase signaling pathways underlying activity-dependent actin remodeling at dendritic spines, Cytoskeleton (Hoboken) 69 (2012) 545–554.
[35] S.P. Fortin, M.J. Ennis, C.A. Schumacher, et al., Cdc42 and the guanine nucleotide exchange factors Ect2 and trio mediate Fn14-induced migration and invasion of glioblastoma cells, Mol. Cancer Res. 10 (2012) 958–968.
[36] E. Malchinkhuu, K. Sato, T. Maehama, et al., S1P(2) receptors mediate inhibition of glioma cell migration through Rho signaling pathways independent of PTEN, Biochem. Biophys. Res. Commun. 366 (2008) 963–968.
[37] L. Goldberg, Y. Kloog, A Ras inhibitor tilts the balance between Rac and Rho and blocks phosphatidylinositol 3-kinase-dependent glioblastoma cell migration, Cancer Res. 66 (2006) 11709–11717.
[38] M. Paez-Ribes, E. Allen, J. Hudock, et al., Antiangiogenic therapy elicits malignant progression of tumors to increased local invasion and distant metastasis, Cancer Cell 15 (2009) 220–231.